SUST Journal of Science and Technology

journal homepage: https://journals.sust.edu

SUST JOURNAL OF SCIENCE AND TECHNOLOGY

# Remote sensing-based assessment of forest loss and fragmentation in Bhawal National Park, Bangladesh

Mohammad Redowan[a,*], Asif Alvee Khan[a], Kanan Akbar Hossain[b], Nusrat Islam[a]

[a] *Department of Forestry & Environmental Science, Shahjalal University of Science & Technology (SUST), Sylhet – 3114, Bangladesh*
[b] *Department of Land, Environment, Agriculture and Forestry, University of Padova, Italy*

ARTICLE INFO

*Keywords:*

LULC
Deforestation
Degradation
Fragmentation
Industrialization

ABSTRACT

Bhawal National Park (BNP), located in central Bangladesh, is a key ecological region that has experienced significant degradation over recent decades due to industrial expansion and increasing human settlement. This study uses geospatial analysis of Landsat satellite imagery from 1990 to 2020 to investigate patterns of deforestation, forest degradation, and fragmentation within the park. A post-classification comparison approach, incorporating a random forest algorithm, was applied, followed by a forest fragmentation assessment using the Landscape Fragmentation Tool. The results reveal substantial changes in land cover over the study period. Dense forest area decreased by 225.45 hectares (24.9%), and medium forest by 485.01 hectares (31.6%), while industrial and urban areas expanded dramatically, surging from 18 ha (0.19%) in 1990 to 1,329 ha (13.97%) in 2020, reflecting an extraordinary annual growth rate of 240.46%. Although the park gained 762.21 hectares of forest, it simultaneously lost 1,655.73 hectares of other forest types. Forest fragmentation intensified, with the number of forest patches nearly doubling, leading to significant changes in patch distribution, edge conditions, and perforated forests, further impacting the park's ecological stability. The study integrates a Socio-Ecological Systems (SES) framework to inform restoration and conservation planning. The results might help inform policy action and strategic management to protect the park's ecological integrity, providing essential guidance for sustainable forest conservation in Bangladesh.

## 1. Introduction

Protected areas serve as institutions that regulate the use of natural resources within defined boundaries [1, 2] and are delineated at various organizational, temporal, and spatial scales [3]. They are widely recognized as essential policy instruments for biodiversity conservation [4], reducing deforestation, maintaining ecological integrity, and mitigating the impacts of climate change [5, 6]. BNP stands out as a crucial protected area among the 51 protected areas in Bangladesh, owing to its ecological, economic, and social significance. Located near the capital city of Dhaka, the park is characterized by tropical moist deciduous forest, predominantly composed of inland Sal trees (*Shorea robusta*) [7]. It hosts a variety of endemic plant and animal species [8], playing a vital role in sustaining local biodiversity and ecological balance. BNP's unique significance is further underscored by its proximity to urban areas, serving as a nature-based recreational zone for city residents and regional visitors [9]. Additionally, it acts as an urban forest, influencing the local microclimatic environment [10]. Recognizing its ecological importance, the area was designated a national park to safeguard its distinctive floral and faunal resources [11, 12] and is listed under the IUCN management category to preserve its ecological features [12].

Over the past few decades, BNP has experienced significant disturbances from various anthropogenic activities [8].

[*] Corresponding author.
*E-mail address:* redowan-for@sust.edu (M. Redowan)

https://doi.org/10.63512/sustjst.2025.1005
Received 1 September 2025; Received in revised form 22 April 2026; Accepted 11 May 2026

The expansion of industrial urbanization and residential development has led to considerable deforestation and forest degradation [12, 13, 14]. A substantial portion of the park's land has been converted into industrial zones, residential areas, and agricultural fields [15]. To date, around 355 industries have been established within the BNP area, with a significant amount of forest land illegally appropriated for these developments [11]. This has resulted in the rapid decline of biodiversity and forest resources [9, 16]. For instance, the capped langur (*Trachypithecus pileatus*), once abundant in this area, is now listed as an endangered species by the IUCN due to habitat loss and degradation [8]. Among all protected areas in Bangladesh, BNP currently faces the most severe threats [17].

Protected areas play a crucial role in ecosystem conservation, yet they also function as complex SES where human activities exert significant influence on ecological stability and management [18]. SES are dynamic and interdependent, with social and ecological components interacting across multiple scales to impact sustainability outcomes [18, 19]. Recent ecological research has underscored the importance of evidence-based conservation and management strategies that account for both ecological and social factors to enhance the success of protected areas [1, 20, 21]. The SES framework is particularly valuable in this context, as it facilitates the evaluation of trade-offs between ecological and social objectives—such as biodiversity conservation versus livelihood needs—and helps in setting realistic management goals [22, 18]. Furthermore, the SES framework enhances the identification of conservation strategies that benefit both ecosystems and local communities, while improving the reliability of evidence used to assess conservation outcomes [23].

Common methodologies for assessing the effectiveness of protected area conservation include monitoring biodiversity—through metrics such as species richness and the presence of indicator species—as well as evaluating land conversion rates, often through remote sensing analysis [24, 25]. As such, periodic assessments of land use and land cover (LULC) changes are essential to discern the patterns and processes driving deforestation, degradation, and forest fragmentation. Forest fragmentation refers to the division of large, continuous forest areas into smaller, isolated patches, typically resulting from human activities such as road construction, agriculture, or urban development. Historical remote sensing data, coupled with geographic information systems, have been widely applied to analyze ecosystem dynamics and elucidate the social and biophysical factors influencing these changes [26, 27]. These technologies provide accurate, comprehensive, and cost-effective quantitative insights for mapping and monitoring the spatial and temporal dynamics of LULC changes [28]. In particular, freely accessible optical Landsat imagery, offering moderate-to-high spatial resolution, enables robust mapping and characterization of LULC changes over large spatial extents [29, 30]. However, there remains a paucity of studies that apply geospatial techniques to accurately quantify deforestation, forest degradation, and fragmentation in BNP. Most current research relies on qualitative assessments to describe the impacts of industrial urbanization on BNP [7, 9, 12], without providing precise spatial or quantitative data. This lack of quantitative and spatial analysis hinders the ability to assess the extent and patterns of forest loss, degradation, and landscape fragmentation over time. Moreover, no studies have integrated geospatial data with SES frameworks, which are essential for understanding the complex interactions between human activities and forest ecosystems. The limited use of such evidence-based frameworks restricts the development of effective, science-driven management strategies to ensure the long-term sustainability and resilience of BNP's forest resources.

The present study aims to address critical gaps in understanding LULC dynamics in BNP by employing geospatial methodologies to quantify changes over the last 30 years (1990–2020) using Landsat time-series imagery. Ten-year intervals (1990–2000–2010–2020) were chosen to capture significant trends in land-use and land-cover change in BNP. The objectives of the research are threefold: (1) to quantitatively assess deforestation and forest degradation, (2) to evaluate forest fragmentation patterns, and (3) to develop a comprehensive, data-driven SES framework that integrates key indicators such as forest degradation, fragmentation, industrialization, and other LULC changes, to inform sustainable management and conservation efforts.

## 2. Study site

Geographically, BNP is located approximately 40 kilometers north of Dhaka, the capital city of Bangladesh, and 13 kilometers northwest of the Gazipur district, at coordinates 24°01′N latitude and 90°20′E longitude [7]. The forest is also known as Bhawal Sal Forest or colloquially as Rajendrapur Gajari Forest. The landscape is characterized by a complex network of depressions arranged in a honeycomb pattern. These depressions, which are privately owned, are typically used for paddy cultivation [31]. The forested area is interspersed with homesteads and cultivable land, collectively covering approximately 9,520 hectares.

This expanse of forest was designated as a national park in 1982, encompassing 5,022 hectares, and was classified as a Protected Landscape/Seascape under Category V of the IUCN classification [11]. The park is managed under two forest ranges: the Bhawal forest range and the national park range [12]. The Bhawal forest range includes the areas of Bhabanipur, B.K. Bari, Rajendrapur West, and Baroipara, while the national park range covers Park Beat, Baupara, and Bankharia (Fig. 1). For management purposes, the forest is divided into two zones: a core zone and a buffer zone. The region is home to a diverse array of flora, with a total of 221 plant species, including 46 tree species, 24 climbers, 19 shrubs, 105 herbs, and 27 types of grass [32, 33]. In addition, the forest provides habitat for approximately 220 vertebrate species, comprising 12 amphibians, 25 reptiles, 148 birds, and 35 mammals [31]. The BNP area strictly prohibits land conversion for industrial purposes, forest product extraction, and the planting of exotic species. However, the park is increasingly subjected to anthropogenic pressures due to its proximity to Dhaka, rapid population growth, and the expansion of large and heavy industries, such as ready-made

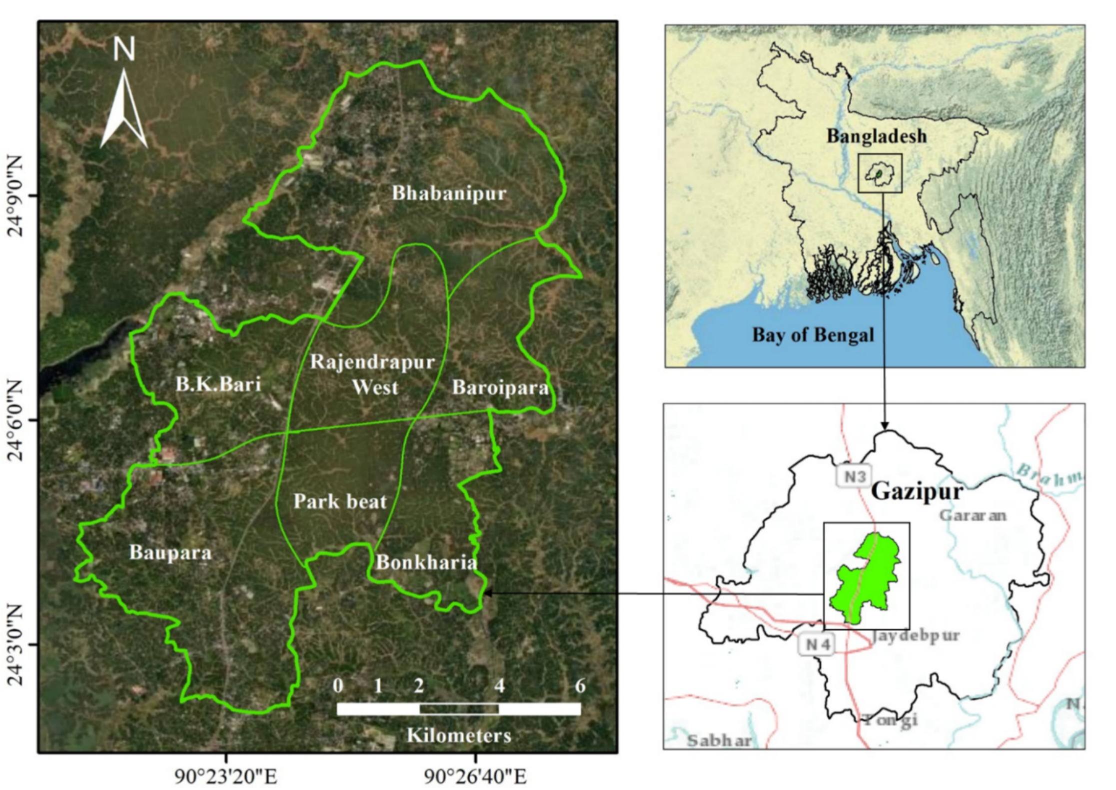


**Figure 1.** Location of Bhawal National Park (BNP) at Gazipur district in Bangladesh

garments and tannery plants, in and around the protected area [17].

## 3. Methodology

The overall methodological framework of the study has been presented in Fig. 2. Initially, the satellite images acquired were classified using a supervised classification approach, employing the random forest algorithm. Following this, the LULC classes were analyzed using trajectory matrices in ArcGIS Pro 3.2. Subsequently, the LULC classes were reclassified into forest and non-forest areas to detect forest fragmentation using the Landscape Fragmentation Tool. Finally, deforestation and fragmentation were analyzed through spatial and statistical approaches. Detailed descriptions of each methodological step are provided in the subsequent sections.

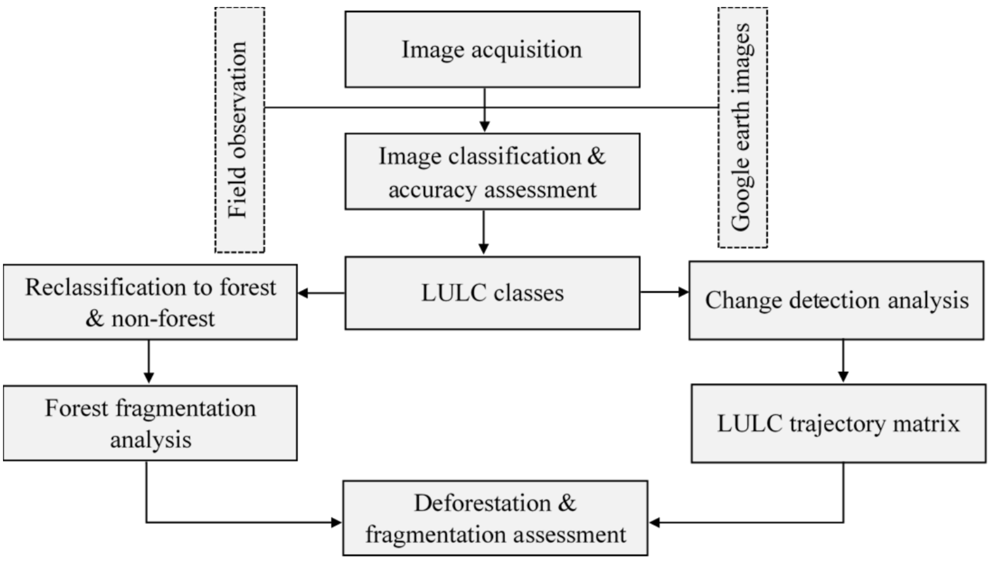


**Figure 2.** Overall methodological framework of the study

### 3.1. Image acquisition

Four cloud-free Landsat images from 1990, 2000, 2010, and 2020 were obtained from the United States Geological Survey web portal for analysis. To reduce seasonal and phenological variations, all images were selected from December, corresponding to the cold-dry season [29]. The spatial resolution and specifications of these images are listed in Table 1. Atmospheric and radiometric corrections of the collected images were performed using Fast Line-of-sight Atmospheric Analysis of Hypercubes (FLAASH) in ENVI 5.3 [29]. Subsequently, the images were subset to the area of interest and registered to a common UTM Zone 46N projection using WGS 84 parameters.

**Table 1.** Characteristics of the Landsat images used for the study

| Study year | Acquisition date | Satellite/ sensors | Path/ Row | Spatial resolution | Used band | False-color composite | | |
|---|---|---|---|---|---|---|---|---|
| | | | | | | R | G | B |
| 1990 | 09-12-1990 | Landsat 5/TM | 137/43 | 30 m | 1–8 | 5 | 4 | 3 |
| 2000 | 20-12-2000 | Landsat 5/TM | 137/43 | 30 m | 1–8 | 5 | 4 | 3 |
| 2010 | 16-12-2010 | Landsat 5/TM | 137/43 | 30 m | 1–8 | 5 | 4 | 2 |
| 2020 | 27-12-2020 | Landsat 8/OLI | 137/43 | 30 m | 1–7 | 6 | 5 | 4 |

### 3.2. Image classification

The images were classified to generate LULC maps using a Random Forest (RF) algorithm in QGIS 3.32 with the Dzetsaka plugin. RF is widely used in vegetation remote sensing for its effectiveness in mapping degraded and fragmented landscapes [34, 35, 36]. Its strength lies in handling nonlinear data and providing accurate predictions, making it superior to methods like Support Vector Machine and Neural Networks, and traditional techniques like Maximum Likelihood [36, 37]. RF is also advantageous for its insensitivity to parameter settings and its ability to determine the relative importance of input variables [38]. It operates by generating multiple decision trees using random subsets of attributes and training data, with each tree voting for the final classification [26, 39].

Six LULC classes were defined: agricultural area, dense forest, medium forest, industrial/urban area, waterbody, and homestead vegetation. Interpretation keys for each class were developed using the natural features of the study site, normalized difference vegetation index (NDVI) values (Table 2), visual interpretation of each LULC class using Google Earth's historical imagery, and field observations (Fig. 3).

NDVI is a widely used metric for monitoring vegetation health, with values ranging from 0 (no vegetation) to 1 (dense vegetation). For medium vegetation and dense vegetation, NDVI values typically range from 0.2 to 0.4 and 0.6 to 1, respectively [40, 41]. NDVI values for the BNP area were classified into non-vegetated areas (with index values from −1 to 0.19, covering water, agricultural areas, and industrial/urban areas) and vegetated areas (with values from 0.2 to 0.54) (Table 2). NDVI for the Landsat images was calculated using the formula provided by [42].

For classification, four cloud-free Landsat 8 and Landsat 5 satellite images were selected to delineate the training samples for the RF models. Polygon-type shapefiles were created with the "ID" and "class" columns in their attribute tables, corresponding to the LULC classes. Training and evaluation of the RF model for supervised classification were performed using accurate ground truth data collected from field surveys [43]. Field-collected location points were imported into QGIS to create a reliable ground truth dataset. High-resolution Google Earth imagery and various combinations of Landsat bands were used to manually draw polygons corresponding to the same land cover as the ground truth points. 150 training samples were created for each study year, amounting to a total of 600 training samples across the four study years, with 25 training samples allocated to each LULC class. Previous research by Abdullah et al. (2019) [44] suggested that selecting an equal number of training samples for each LULC class reduces the influence of majority versus minority classes on the RF algorithm. The final image classification using the RF algorithm produced LULC maps containing the designated classes for each image.

### 3.3. Accuracy assessment

Accuracy assessment is a crucial step in the classification process [45, 46]. In this study, 550 reference points were selected using a stratified random sampling technique via ArcGIS's sampling design tool, ensuring proportional representation of all six LULC classes. These same 550 points were applied to each study year's classified images to measure accuracy, resulting in a total of 3,300 reference points checked over the four study years. High-resolution Google Earth images and field surveys were used to validate these points [47]. Points that were too close to the boundary of two different land cover classes were slightly adjusted to ensure they represented a full Landsat pixel [29].

The classification accuracy was evaluated by calculating error metrics, including producer, user, and overall accuracy, as well as the Kappa coefficient [48, 49]. The Kappa coefficient ranges from −1 to 1, with a value of 1 indicating perfect agreement, and values close to 0 or negative indicating that the agreement is worse than would be expected by chance [50]. A higher Kappa value signifies a higher accuracy of the LULC classification.

### 3.4. Deforestation and degradation analysis

The changes in LULC trajectories were obtained using the post-classification comparison method, the most widely

**Table 2.** LULC classification scheme used to analyze degradation and forest fragmentation

| LULC class | Description | NDVI value | Reclass |
|---|---|---|---|
| Dense forest | Natural Sal and plantation forest. Dense forest cover represents areas where the number of trees is higher than 200 per ha. | >0.40 | Forest |
| Medium forest | Natural Sal and plantation forest. Medium forest cover represents areas where the number of trees is less than 200 per ha. | 0.20–0.40 | Forest |
| Agricultural area | All cultivated and uncultivated agricultural areas such as paddy fields, farmlands, crop fields including fallow lands, barren, areas most often represent bare soil. | <0.20 | Non-forest |
| Homestead vegetation | Fruit trees, private forest (multipurpose trees), vegetables, fodder, fuelwood, and ornamental herbs/shrubs. | <0.20 | Non-forest |
| Industrial/Urban area | Commercial and socio-economic industries, multistoried residential buildings, tin-shed houses, highway roads, small shops beside roads, transportation, and other sub roads. | <0.10 | Non-forest |
| Waterbody | Seasonal open water, ponds, lakes, reservoirs, and any type of water surface. | <0 | Non-forest |

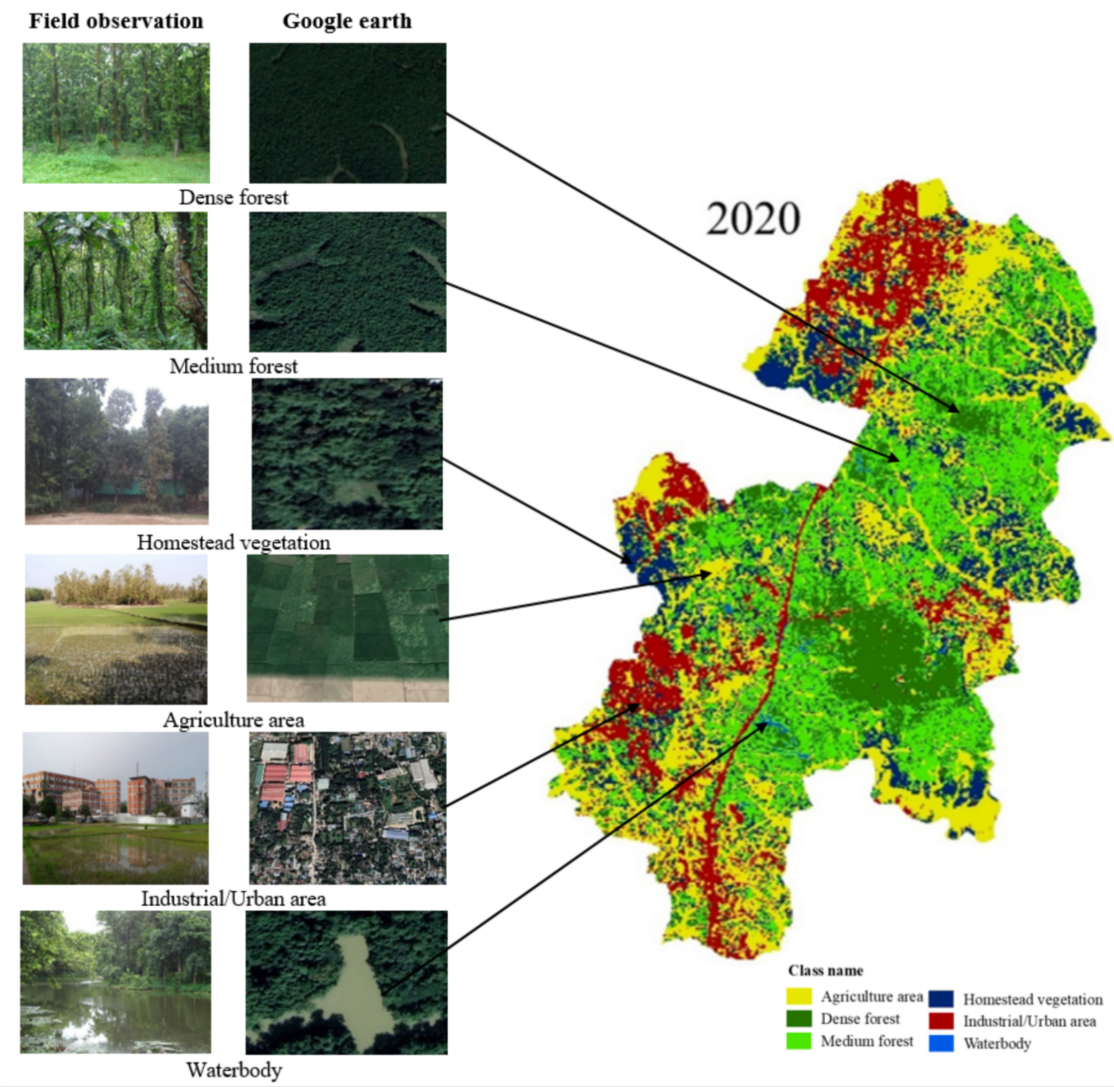


**Figure 3.** LULC image classification using Google Earth's historical images and field observations (2020)

used technique for detecting changes in LULC classes from classified images despite some limitations [51]. This method provides detailed "from-to" information on LULC changes [52, 53] and helps detect and assess land cover loss and degradation through LULC trajectory matrices, revealing periodic transitions [54, 55]. Applied to all classified images in the time-series, it generated cross-tabulation matrices using ArcGIS overlay functions [55], allowing for the

**Table 3.** Classes of landscape fragmentation tool for subsequent analysis

| Classes | Descriptions |
|---|---|
| Patch Forest | A pixel represents a small forested area surrounded by non-forested land cover. |
| Edge Forest | Pixel represents the boundary between core forest and large non-forested land cover features (using a specified edge width of 100 m). |
| Perforated Forest | Pixel represents the boundary between the core forest and relatively small clearings (perforations) within the forested land (interior edges along with small gaps in the forest). |
| Core Forest | Forest pixels that are comparatively far from the forest–non forest boundary. It is forested areas bounded by more forested regions. |
| Non-forest | Non-forested areas include industry, settlement, agricultural area, bare land, and non-forested wetlands. These areas, along with developed land, are considered fragmenting features. |

calculation of transitions and degradations in LULC during 1990–2000, 2000–2010, 2010–2020, and 1990–2020.

### 3.5. Fragmentation analysis

The level of fragmentation within BNP was analyzed using fragmentation indices and maps generated by the Landscape Fragmentation Tool [56]. This tool has been reported to outperform other similar tools, such as FRAGSTATS, as it provides both a graphical representation of data through raster maps and quantitative insights [57]. In contrast, FRAGSTATS, also known as the patch analyst, primarily offers quantitative information without the accompanying visual representation [58].

For the fragmentation analysis, each classified image was reclassified in ArcGIS into two categories: forest (including dense and medium forest) and non-forest (including industrial/urban areas, agricultural areas, homestead vegetation, and water bodies), which is a prerequisite for using the tool [56]. The data were inputted into the tool in raster format; with non-forest areas assigned a value of 1 and forest areas a value of 2. Fragmentation maps were then prepared, using a 100-meter edge as the default value because it is a widely accepted threshold in landscape ecology for distinguishing core from edge habitats. This distance effectively captures edge effects—such as microclimate changes, increased exposure to invasive species, and human disturbances—that typically occur within 100 meters of the forest boundary. It also standardizes results for comparison with similar studies and supports ecologically meaningful conservation planning [17, 58]. The various classes of fragmentation are detailed in Table 3.

To assess changes in the spatial and temporal patterns of the study area, landscape indices were calculated using the Patch Analyst 4.0 extension in ArcGIS. The indices included Class Area, Number of Patches, Mean Patch Size, Area-Weighted Mean Shape Index, and Edge Density [59, 60]. Class Area represents the total area occupied by all patches of a specific land cover class, providing insight into the extent of each land cover type [61]. Number of Patches denotes the total number of patches within a class or across the landscape, helping to understand landscape transformation processes. Mean Patch Size, the average size of patches within a class, serves as an accurate predictor of patch diversity [62]. Area-Weighted Mean Shape Index reflects patch shape complexity and diversity, calculated as the sum of each patch's shape value weighted by its proportional abundance. Edge Density measures the amount of edge relative to the total landscape area, indicating spatial heterogeneity and edge effects on biodiversity [61]. These indices collectively provide a comprehensive view of landscape patterns, fragmentation, and ecological impacts.

## 4. Results

### 4.1. Deforestation and degradation

The accuracy of image classification for producing LULC, deforestation, and degradation maps were high, ranging from 88% to 91%. The overall accuracies of the classified images for the years 1990, 2000, 2010, and 2020 were 89%, 92%, 88%, and 91%, respectively, with corresponding kappa values of 0.87, 0.90, 0.85, and 0.89 (Table 4). The corresponding producer's and user's accuracies were also notably high (Table 4).

The spatiotemporal analysis of LULC reveals substantial changes over the past 30 years, with notable shifts occurring particularly after 2000, driven by industrial and urban expansion. Most industrial and urban development has concentrated in the western and southwestern regions of the park (Fig. 4).

In 1990, the primary land covers were agriculture (48.44%) and forest areas (47.76%), encompassing both dense and medium forest types, with homestead vegetation (3.35%), water bodies (0.26%), and industrial/urban areas (0.19%) comprising the remainder (Table 5). However, the dense forest area experienced an annual decrease of 1.37% from 1990 to 2020, with the most pronounced decline of 2.21% occurring between 1990 and 2000. Although medium forest cover exhibited variability over time (Fig. ??), the overall trend shows a decline, with a minor increase observed between 1990 and 2000. Conversely, homestead vegetation and industrial/urban areas saw dramatic increases, with homestead vegetation rising from 3.35% (318.78 ha) in 1990 to 17.31% (1647.54 ha) in 2020, and industrial/urban areas expanding from 0.19% (18.18 ha) to 13.97% (1329.66 ha) over the same period. Notably, industrial/urban areas experienced the highest annual increase rate of 240.46% compared to other LULC classes from 1990 to 2020 (Table 5).

The LULC transitions at BNP between 1990 and 2020 were spatially and temporally very dynamic (Fig. 5 and Table 6). Over this period, 370.5 hectares transitioned from other land classes to dense forest, while 1109.79 hectares of

**Table 4.** Distribution of accuracy metrics of classified Landsat images (1990–2020)

| Year | LULC classes | | | | | | | | | | | | Overall accuracy (%) | Kappa coefficient |
|---|---|---|---|---|---|---|---|---|---|---|---|---|---|---|
| | Dense forest | | Medium dense forest | | Waterbody | | Homestead vegetation | | Industrial/ Urban area | | Agricultural area | | | |
| | PA | UA | PA | UA | PA | UA | PA | UA | PA | UA | PA | UA | | |
| 1990 | 81 | 91 | 90 | 88 | 100 | 90 | 84 | 79 | 91 | 89 | 93 | 96 | 89 | 0.87 |
| 2000 | 84 | 91 | 91 | 90 | 100 | 87 | 90 | 86 | 92 | 96 | 95 | 96 | 92 | 0.90 |
| 2010 | 74 | 78 | 88 | 82 | 100 | 87 | 81 | 81 | 85 | 94 | 94 | 95 | 88 | 0.85 |
| 2020 | 81 | 81 | 88 | 87 | 100 | 93 | 87 | 89 | 96 | 97 | 97 | 98 | 91 | 0.89 |

"PA" and "UA" indicate the producer's and user's accuracy (%), respectively.

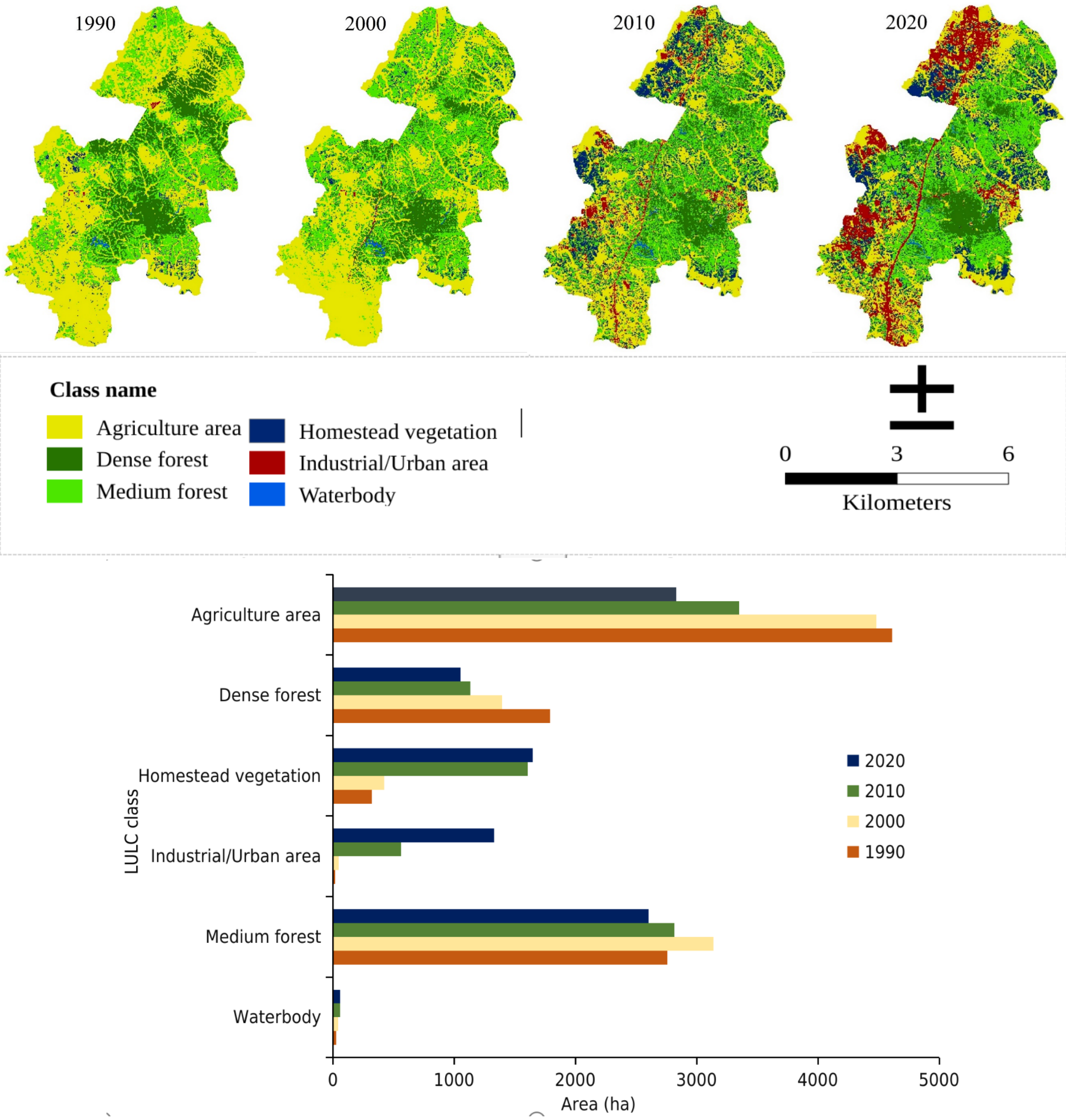


**Figure 4.** LULC change map of BNP from 1990 to 2020

dense forest converted to other land uses. In the medium-dense forest category, 1551.87 hectares were added from other classes, and 1706.40 hectares were lost to other land uses.

**Table 5.** LULC change statistics of BNP (1990–2020)

| Class name | Area (ha) (% of total area) | | | | Area changes (ha) (Annual rate of changes %) | | | |
|---|---|---|---|---|---|---|---|---|
| | 1990 | 2000 | 2010 | 2020 | 1990–2000 | 2000–2010 | 2010–2020 | 1990–2020 |
| Dense forest | 1789.83 (18.80) | 1394.19 (14.64) | 1133.82 (11.91) | 1050.84 (11.04) | −395.64 (−2.21) | −260.37 (−1.87) | −82.98 (−0.73) | −738.99 (−1.37) |
| Medium forest | 2756.97 (28.96) | 3136.86 (32.95) | 2813.76 (29.56) | 2602.44 (27.34) | +379.89 (+1.38) | −323.10 (−1.03) | −211.32 (−0.75) | −154.53 (−0.19) |
| Waterbody | 24.30 (0.26) | 43.29 (0.45) | 57.60 (0.61) | 58.14 (0.61) | +18.99 (+7.81) | +14.31 (+3.30) | +0.54 (+0.09) | +33.84 (+4.64) |
| Homestead vegetation | 318.78 (3.35) | 421.29 (4.43) | 1604.52 (16.85) | 1647.54 (17.31) | +102.51 (+3.22) | +1183.23 (+28.09) | +43.02 (+0.27) | +1328.76 (+13.90) |
| Industrial/Urban area | 18.18 (0.19) | 44.82 (0.47) | 559.71 (5.88) | 1329.66 (13.97) | +26.64 (+14.65) | +514.89 (+114.88) | +769.95 (+13.75) | +1311.48 (+240.46) |
| Agriculture area | 4611.96 (48.44) | 4479.57 (47.00) | 3350.61 (35.20) | 2831.40 (29.74) | −132.39 (−0.29) | −1128.96 (−2.52) | −519.21 (−1.55) | −1780.56 (−1.29) |

"+" and "−" indicate an increase and decrease, respectively.

In 1990, the stable dense forest area was 905.49 hectares, which diminished to 680.04 hectares by 2020. Similarly, the stable medium forest area decreased from 1535.58 hectares in 1990 to 1050.57 hectares in 2020. The industrial/urban areas exhibited the most substantial increase, expanding from 18.18 hectares in 1990 to 1329.66 hectares in 2020. Notably, the conversion of dense and medium-dense forests to industrial/urban areas was particularly pronounced between 2010 and 2020, reflecting a more significant shift during this period compared to previous decades (Table 6).

The BNP has experienced persistent deforestation and forest degradation over the past decades. Between 1990 and 2020, the park saw an increase of approximately 762.21 hectares in forested areas, while 1655.73 hectares were deforested. By the end of this period, stable forest areas amounted to 2891.07 hectares, contrasted with 4211.01 hectares of stable non-forest areas (Fig. 6).

Throughout the study period, gradual forest degradation was evident (Fig. 7). Specifically, in 2020, the stable dense forest and medium-dense forest areas were 680.04 hectares and 1050.57 hectares, respectively. During this time, 888.75 hectares of dense forest were converted to medium forest, whereas 271.71 hectares of medium forest were transformed into dense forest.

### 4.2. Forest fragmentation

Forest fragmentation patterns for BNP were analyzed for 1990 and 2020 using the Landscape Fragmentation Tool. The fragmentation maps, categorized into patch, edge, perforated, core, and non-forest areas, are presented in Fig. 8, with detailed statistics in Tables 7 and 8.

The dense forest (core), the most significantly affected class, increased from 10.19% (463.23 ha) in 1990 to 14.96% (546.48 ha) in 2020. The overall forest area declined by approximately 893.52 ha, which also altered the fragmentation classes. The patch forest decreased slightly from 1036.98 ha to 853.65 ha between 1990 and 2020. Edge and perforated forests were dominant during the study period. The edge forest decreased from 32.67% (1485.54 ha) in 1990 to 31.65% (1156.14 ha) in 2020, while the perforated forest reduced from 34.33% (1561.05 ha) to 30.03% (1097.01 ha) (Table 7).

From 1990 to 2020, the number of forest patches nearly doubled from 1313 to 2278, while the number of non-forest patches decreased from 1672 to 1122 (Table 8). The findings indicate a significant decline in the mean patch size for the forest class (from 3.46 ha to 1.60 ha), whereas it increased for the non-forest class (from 2.97 ha to 5.23 ha). Additionally, edge density declined for both forest and non-forest classes during the study period (Table 8).

**Table 7.** Forest fragmentation change from 1990–2020

| Fragmentation class | Area (ha) 1990 | % of area | Area (ha) 2020 | % of area |
|---|---|---|---|---|
| Patch | 1036.98 | 22.81% | 853.65 | 23.37% |
| Edge | 1485.54 | 32.67% | 1156.14 | 31.65% |
| Perforated | 1561.05 | 34.33% | 1097.01 | 30.03% |
| Core | 463.23 | 10.19% | 546.48 | 14.96% |
| Total | 4546.80 | | 3653.28 | |

**Table 8.** Fragmentation patch indices from 1990–2020

| Class name | 1990 Forest | 1990 Non-forest | 2020 Forest | 2020 Non-forest |
|---|---|---|---|---|
| Number of Patches | 1313 | 1672 | 2278 | 1122 |
| Mean Patch Size | 3.46 | 2.97 | 1.60 | 5.23 |
| Mean Shape Index | 1.40 | 1.33 | 1.28 | 1.33 |
| Edge Density | 117.42 | 120.59 | 106.15 | 111.40 |
| Area Weighted Mean Shape Index | 12.56 | 13.76 | 11.29 | 15.09 |
| Class area (ha) | 4546.80 | 4973.22 | 3653.28 | 5866.74 |

## 5. Discussion

### 5.1. Deforestation and degradation

The overall image classification accuracies and corresponding kappa coefficients were high, indicating a strong level of agreement with the validation data [63, 50]. The high accuracy obtained can be attributed to the adequate

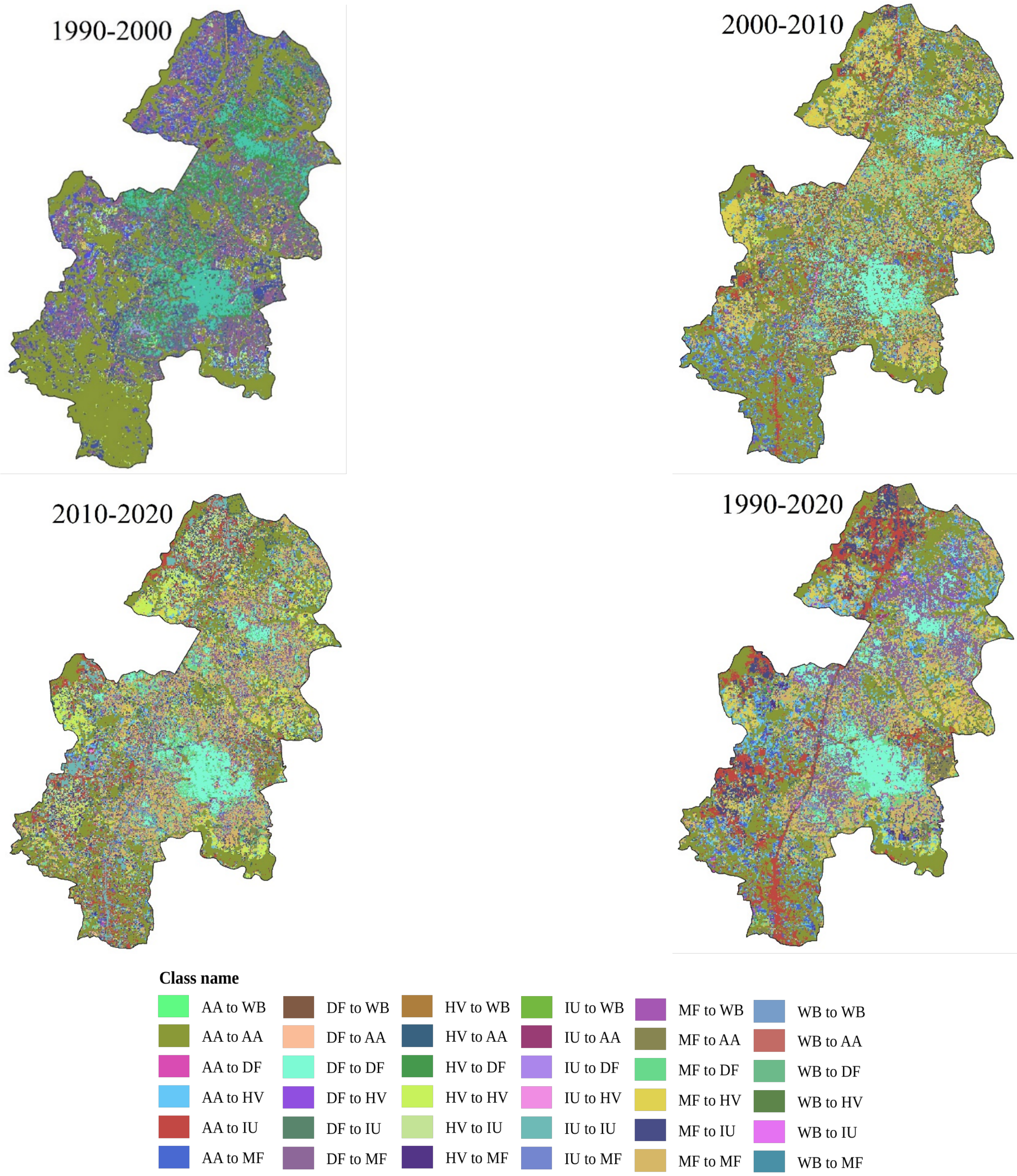


**Figure 5.** LULC change trajectories of BNP from 1990 to 2020

number of training samples and field observations used during the LULC classification process. A sufficient number of training samples is crucial for accurate land cover classification, which enhances the overall classification accuracy [64]. Additionally, the use of the Random Forest classifier, which is more effective than traditional methods like Maximum Likelihood [30, 34], contributed to the improved accuracy. The disparity between producers' and user's accuracies was less for agricultural and industrial/urban areas compared to other LULC classes. This is likely due to the distinct spectral characteristics of agricultural and industrial/urban areas, which differentiate them more clearly from other land cover types such as dense and medium forest.

BNP has experienced significant transformations over the study period, notably marked by extensive conversion of land to industrial and residential uses. From 1990 to 2020, the area dedicated to homestead vegetation and in-

**Table 6.** LULC change trajectory matrices of BNP (1990–2020). Bold diagonal values indicate stable (unchanged) areas.

| Period | Class name | AA (ha) | DF (ha) | HV (ha) | IU (ha) | MF (ha) | WB (ha) | Total (ha) |
|---|---|---|---|---|---|---|---|---|
| 1990–2000 | AA | **3601.26** | 63.99 | 189.27 | 20.97 | 724.50 | 11.97 | 4611.96 |
| | DF | 114.66 | **905.49** | 17.28 | 9.00 | 732.42 | 10.98 | 1789.83 |
| | HV | 121.41 | 15.48 | **39.42** | 0.18 | 142.20 | 0.09 | 318.78 |
| | IU | 12.87 | 0.54 | 0.18 | **3.42** | 0.81 | 0.36 | 18.18 |
| | MF | 623.43 | 406.71 | 175.14 | 8.91 | **1535.58** | 7.20 | 2756.97 |
| | WB | 5.94 | 1.98 | 0.00 | 2.34 | 1.35 | **12.69** | 24.30 |
| | Total | 4479.57 | 1394.19 | 421.29 | 44.82 | 3136.86 | 43.29 | 9520.02 |
| 2000–2010 | AA | **2846.79** | 59.94 | 531.18 | 377.82 | 641.07 | 22.77 | 4479.57 |
| | DF | 37.98 | **645.30** | 61.29 | 31.86 | 611.64 | 6.12 | 1394.19 |
| | HV | 90.18 | 8.01 | **181.53** | 16.20 | 125.10 | 0.27 | 421.29 |
| | IU | 14.49 | 2.79 | 0.99 | **13.68** | 8.55 | 4.32 | 44.82 |
| | MF | 356.76 | 413.37 | 828.63 | 114.39 | **1422.45** | 1.26 | 3136.86 |
| | WB | 4.41 | 4.41 | 0.90 | 5.76 | 4.95 | **22.86** | 43.29 |
| | Total | 3350.61 | 1133.82 | 1604.52 | 559.71 | 2813.76 | 57.60 | 9520.02 |
| 2010–2020 | AA | **2088.18** | 31.68 | 419.76 | 534.78 | 257.49 | 18.72 | 3350.61 |
| | DF | 23.67 | **533.43** | 34.83 | 17.73 | 521.46 | 2.70 | 1133.82 |
| | HV | 334.17 | 37.71 | **638.55** | 248.58 | 344.88 | 0.63 | 1604.52 |
| | IU | 105.30 | 10.53 | 23.40 | **364.41** | 50.76 | 5.31 | 559.71 |
| | MF | 267.66 | 434.07 | 530.46 | 160.65 | **1414.08** | 6.84 | 2813.76 |
| | WB | 12.42 | 3.42 | 0.54 | 3.51 | 13.77 | **23.94** | 57.60 |
| | Total | 2831.40 | 1050.84 | 1647.54 | 1329.66 | 2602.44 | 58.14 | 9520.02 |
| 1990–2020 | AA | **2312.37** | 75.78 | 773.37 | 864.45 | 559.26 | 26.73 | 4611.96 |
| | DF | 59.67 | **680.04** | 106.29 | 44.01 | 888.75 | 11.07 | 1789.83 |
| | HV | 62.91 | 21.06 | **99.99** | 37.62 | 96.93 | 0.27 | 318.78 |
| | IU | 9.36 | 0.45 | 2.25 | **1.98** | 2.34 | 1.80 | 18.18 |
| | MF | 382.86 | 271.71 | 664.29 | 378.36 | **1050.57** | 9.18 | 2756.97 |
| | WB | 4.23 | 1.80 | 1.35 | 3.24 | 4.59 | **9.09** | 24.30 |
| | Total | 2831.40 | 1050.84 | 1647.54 | 1329.66 | 2602.44 | 58.14 | 9520.02 |

AA = Agriculture area, DF = Dense forest, MF = Medium forest, HV = Homestead vegetation,
IU = Industrial/Urban area, WB = Waterbody

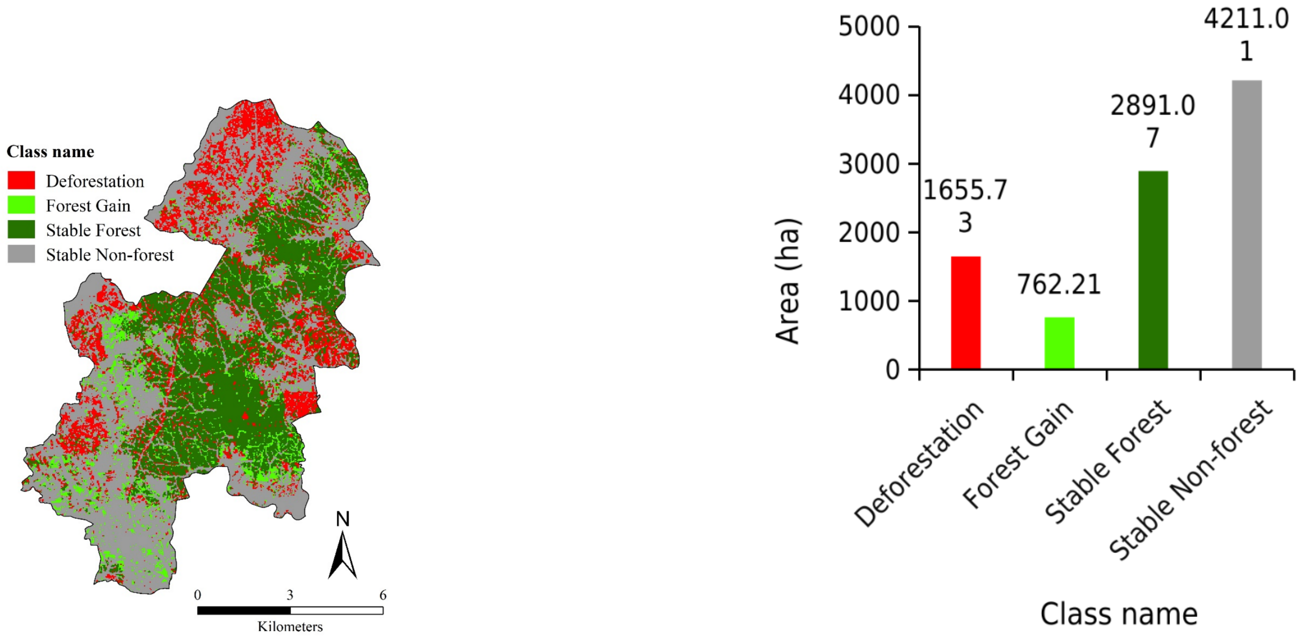


**Figure 6.** Graphical representation of deforestation from 1990 to 2020

dustrial/urban land increased dramatically, from 3.35% and 0.19% to 17.31% and 13.97%, respectively. Approximately 12.6% of BNP is now occupied by permanent industrial settlements [12], and 13.84% of the forest area faces encroachment by individual households [16]. Results indicate that most industrial/urban areas are concentrated near highways traversing the forest, with significant impacts observed in the Bhabanipur, B.K. Bari and Baupara beats, par-

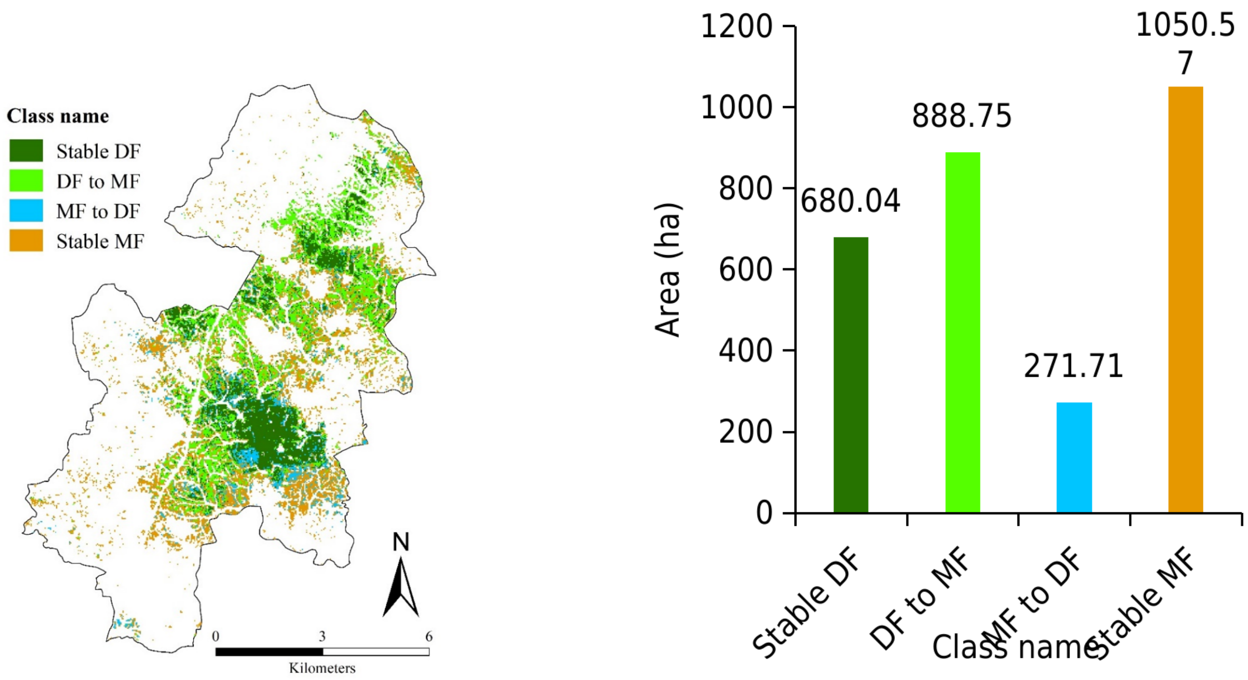


**Figure 7.** Transition map of forest degradation from 1990 to 2020 (DF = Dense forest, MF = Medium forest)

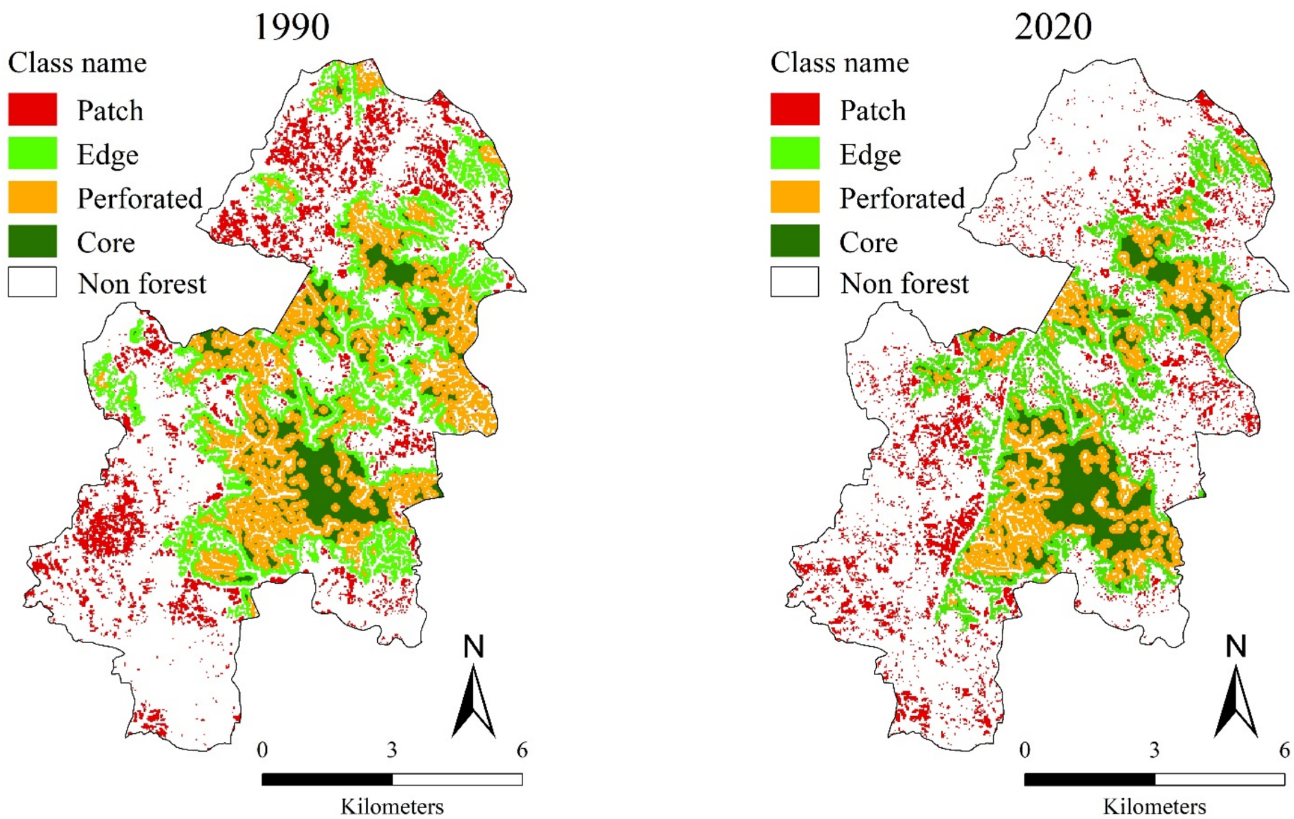


**Figure 8.** Geospatial and graphical representation of forest fragmentation from 1990 to 2020

ticularly in the west and southwest. Notably, about 80% of the industrial/urban-related deforestation occurred in these three beats [12].

The current LULC maps show that the rapid expansion of industrial/urban areas, especially after 2000, has led to a substantial decline in forest cover and an increase in non-forest areas (Fig. 9). Initially, dense and medium forests, along with agricultural lands, were the predominant LULC classes. However, the forest area has gradually diminished due to the encroachment of industrial/urban developments. Approximately 355 industries have emerged within BNP, illegally appropriating significant forest areas [11]. This study highlights that industrialists and influential individuals continue to seize land and build industries within the forest. Despite attempts by the Bangladesh Forest Department to reforest through leasing forest lands to farmers, the approach has not been effective. The park is now encircled by extensive agricultural activities, with a tendency for agricultural workers to encroach further into forested areas during each farming season. Consequently, forest areas adjacent to human activities are at the highest risk of degradation [13, 31]. The most ecologically concerning patterns include the substantial loss of natural habitats, increased fragmentation of contiguous green spaces, and the expansion of built-up or agricultural areas into previously undisturbed ecosystems. These developments threaten biodiversity, diminish ecosystem connectivity, and compromise the resilience of natural systems to environmental stressors. Among all protected areas in Bangladesh, BNP is currently facing the most significant threats, including settlement encroachment, conversion of forest land to agriculture, and industrial activities that cause pollution and ecological disturbance [17].

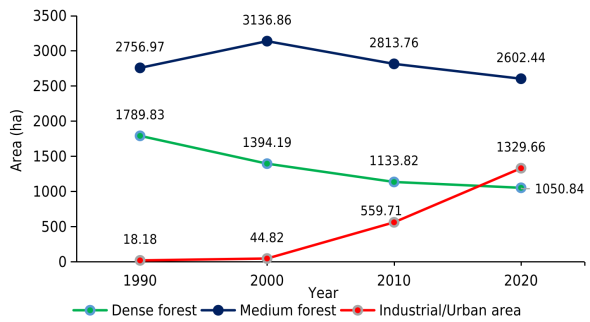


**Figure 9.** Trend of dense forest, medium forest, and industrial/urban area in the study site

### 5.2. Forest fragmentation

In the fragmentation analysis of BNP, the forest area was categorized into four thematic types: patch, edge, core, and perforated. These categories reflect the qualitative and quantitative aspects of forest fragmentation. The results indicate a continued decline in forest patches and an increase in the perforated areas, signifying heightened fragmentation. Notably, the number of forest patches nearly doubled by 2020 compared to 1990, and the average patch size decreased, suggesting an intensification of fragmentation largely driven by edge effects [56]. The proliferation of forest patches indicates increasing disconnection from core forest areas, which is detrimental to habitat continuity [65]. Smaller and more isolated habitat patches generally support fewer species, particularly those requiring extensive territories or possessing limited dispersal capacities. Increased edge density intensifies exposure to external threats such as invasive species, pollution, and microclimatic changes. These factors collectively reduce species richness, disrupt ecological processes, and reduce overall ecosystem health.

Despite various conservation initiatives by the Bangladesh Forest Department that have improved core forest regions and reduced edge effects, the extent of edge and perforated areas remains higher than other types. This reflects ongoing non-forest land use practices within the park. The decrease in forest cover and increase in open forest and forest gaps are indicative of deteriorating forest structure, posing a significant threat to biodiversity [27]. For example, BNP, which once harbored tigers, leopards, and peacocks, has seen the complete disappearance of these species [33]. Additionally, indigenous tree species have largely vanished, replaced by exotic species like *Acacia* spp. and *Eucalyptus* spp. [12].

Industrialization and agriculture have been the primary drivers of fragmentation within BNP. The expansion of infrastructure—including highways, roads, high-voltage transmission lines, gas pipelines, and factories—has led to extensive deforestation. This trend began in the 2006–07 period when the caretaker government issued environmental clearance certificates for industries on privately owned land within BNP, legalizing existing industries and encouraging new developments. The lax enforcement of environmental regulations and governmental favoritism have allowed industrialists and influential individuals to further encroach upon the forest. Without substantial conservation efforts, the situation is likely to deteriorate further.

### 5.3. The SES framework

The SES framework is instrumental in identifying and analyzing the factors influencing outcomes such as forest cover, biodiversity, and ecosystem services, along with their interrelationships [22]. It explores how focal action situations (e.g., enrichment planting) interact with resource systems, governance systems, resource units, and users to shape these outcomes (Fig. 10). Resource systems encompass biophysical factors that maintain landscape composition and structure, such as forest density and agroforestry practices, while governance systems include socio-economic factors governing landscape management and regulation, including forest law and industrial policies. These systems can directly or indirectly impact the focal action situations. Resource units represent land uses and landscape features, such as native flora and fauna, fuel, and fodder, while users are individuals who benefit from the landscape, both directly and indirectly (Fig. 10).

Integrating the SES framework into conservation planning provides a structured approach to incorporating complex local and regional socio-economic factors. This integration involves organizing data to identify and classify factors critical for developing and implementing sustainable conservation plans [66, 67].

This study applies a systematic decision-making process guided by the SES framework to inform the restoration and conservation planning for BNP. The process involves defining primary goals, such as restoring degraded forests to enhance biodiversity and ecosystem services, while considering socio-ecological aspects, including ecological suitability, social and political acceptability, and economic feasibility. It entails building community awareness and planning by engaging relevant stakeholders (e.g., foresters, local communities, industrialists) and considering various sectors (e.g., forestry, agriculture, industry). Specific objectives are identified, such as addressing forest degradation

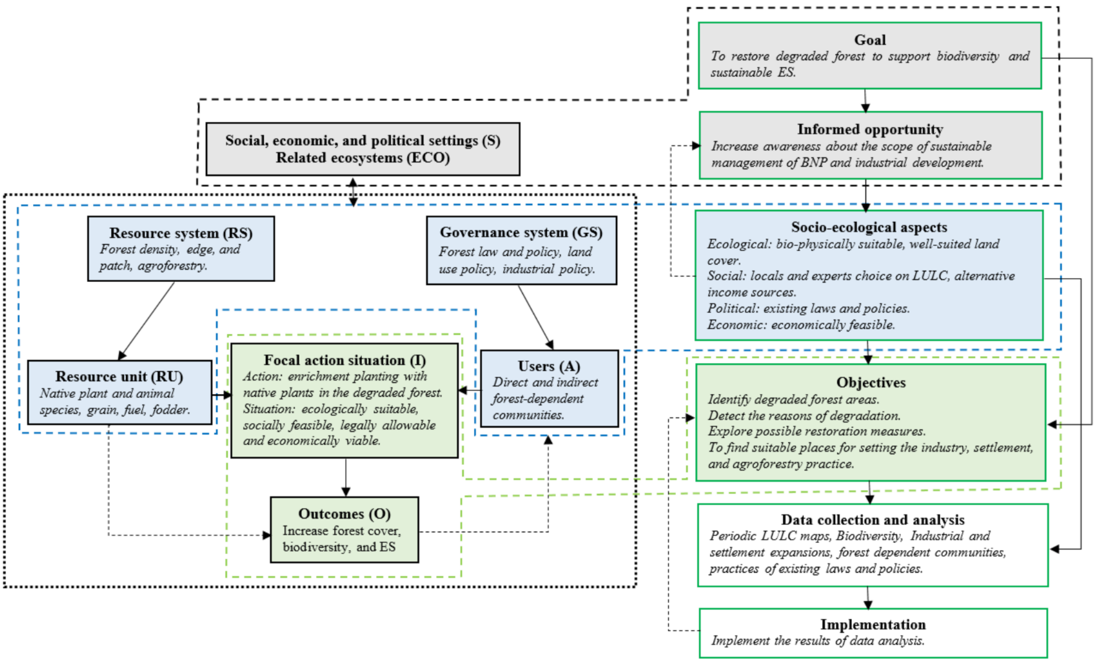


**Figure 10.** Logical SES framework concepts in restoration and conservation planning of the BNP. The black boundary boxes represent the SES framework, adapted from Ostrom (2009) [22], and they show feedback (dashed arrows) and direct links (solid arrows). Green boundary boxes show phases in systematic decision-making, adapted from Budiharta et al. 2016 and Gregory et al. (2012) [66, 67]. Black, blue, and light green dashed boundary boxes show the links between elements of the two frameworks.

and identifying suitable locations for industry and settlement. Evidence-based data, including periodic LULC maps, industrial expansion, and current policies, are collected for analysis to achieve conservation goals and restore BNP. The connections between the SES elements and the systematic conservation planning framework are illustrated with boundary boxes in Fig. 10.

## 6. Conclusions

The ecologically important BNP in Bangladesh has experienced significant degradation over the past few decades due to intensified human activities. This study leverages geospatial analysis of Landsat satellite time-series data, supplemented by field observations, to assess the rapid decline and degradation of BNP's forests. The analysis underscores the role of industrial urbanization as a primary driver of these adverse changes. Freely available Landsat imagery has proven to be a powerful tool for evaluating deforestation, forest degradation, and fragmentation, providing a comprehensive view of the park's evolving landscape.

The study demonstrates a marked reduction in forest cover and a substantial increase in non-forest areas between 1990 and 2020. Specifically, the core zone of the forest has experienced relatively less anthropogenic impact compared to the buffer zone, which has been subjected to significant disturbances. The study highlights a marked increase in forest fragmentation, with a growing number of smaller, isolated patches and a decline in the overall size and continuity of forested areas. This fragmentation threatens the ecological integrity of the park and its ability to support diverse wildlife. Key factors contributing to this impact include industrial development, expansion of settlements, illegal logging, encroachment on forest land, and inadequate administrative oversight. The cumulative effects of these activities have led to profound alterations in the park's landscape, placing its ecological integrity at considerable risk. If current trends continue, BNP's forest ecosystems face an existential threat.

Addressing these challenges necessitates immediate and robust policy interventions and strategic management decisions. Strategic and managerial actions must focus on curbing industrial expansion, preventing illegal activities, and enhancing law enforcement. The SES offers a robust approach for identifying and analyzing the various factors influencing land use and land cover changes. By applying this framework, stakeholders can gain insights into the complex interactions between ecological and socio-economic factors, which are crucial for developing and implementing effective conservation strategies. The framework facilitates a comprehensive understanding of the factors affecting BNP's environment, enabling the formulation of sustainable management strategies that address both ecological and human dimensions. For instance, regular satellite monitoring using remote sensing technologies systematically tracks changes in forest cover and landscape structure over time. This approach enables the timely detection of deforestation, fragmentation, and other land-use changes, thereby supporting data-driven decision-making and early identification of emerging ecosystem threats. In this regard, establishing buffer zones around core forests can mitigate the direct impacts of human activities on ecologically significant areas. Furthermore, allocating industrial development zones away from forest boundaries minimizes habitat disturbance, reduces pollution risks, and preserves ecological connectivity.

The critical insights derived from this study are intended to inform decision-makers, including park managers, policymakers, and the scientific community. It emphasizes the importance of utilizing remote sensing and spatial analysis technologies for cost-effective exploratory planning, scenario development, and impact modeling. These technologies offer valuable tools for assessing current conditions, predicting future trends, and evaluating the effectiveness of conservation measures. By integrating these tools into conservation efforts, stakeholders can enhance their capacity to protect and restore BNP's forest ecosystems, ultimately ensuring the long-term preservation of this vital natural resource.

The findings of this study may help manage protected forests in developing countries like Bangladesh, which are highly affected by anthropogenic disturbances, including industrial and urban development, settlement, and agricultural expansion.

In this study, we utilized freely available Landsat satellite imagery to assess deforestation and fragmentation in the BNP over a decadal period. Future research could incorporate high-resolution lidar imagery for more detailed and frequent assessments of land-use and land-cover dynamics. Subsequent studies should also focus on temporal changes in ecosystem service values with spatio-economic modelling.

**Acknowledgement**

This research was generously funded by the University Grants Commission (UGC) of Bangladesh (Ref No: 37-01-0000-073-04-025/2019/2738). We extend our heartfelt gratitude to the staff of the Bangladesh Forest Department for their unwavering support during the field campaign. Our sincere thanks also go to the anonymous reviewers for their invaluable comments and suggestions, which have greatly enhanced the quality of this manuscript.

**References**

[1] M. Bonilla-Moheno, C. E. Rangel Rivera, E. García-Frapolli, F. L. Ríos Beltrán, C. Espadas-Manrique, F. Aureli, B. Ayala-Orozco, and G. Ramos-Fernández, "Changes in the socio-ecological system of a protected area in the Yucatan Peninsula: A case study on land-use, vegetation cover, and household management strategies," *Land*, vol. 10, no. 11, 2021. https://doi.org/10.3390/land10111147.

[2] T. M. Hayes, "Parks, people, and forest protection: An institutional assessment of the effectiveness of protected areas," *World Development*, vol. 34, pp. 2064–2075, 2006. https://doi.org/10.1016/j.worlddev.2006.03.002.

[3] G. S. Cumming, C. R. Allen, N. C. Ban, D. Biggs, H. C. Biggs, D. H. M. Cumming, A. De Vos, G. Epstein, M. Etienne, K. Maciejewski, R. Mathevet, C. Moore, M. Nenadovic, and M. Schoon, "Understanding protected area resilience: A multi-scale, social-ecological approach," *Ecological Applications*, vol. 25, no. 2, pp. 299–319, 2015. https://doi.org/10.1890/13-2113.1.

[4] S. Chape, J. Harrison, M. Spalding, and I. Lysenko, "Measuring the extent and effectiveness of protected areas as an indicator for meeting global biodiversity targets," *Philosophical Transactions of the Royal Society B*, vol. 360, no. 1454, pp. 443–455, 2005. https://doi.org/10.1098/rstb.2004.1592.

[5] J. Ervin, "Rapid assessment of protected area management effectiveness in four countries," *BioScience*, vol. 53, no. 9, pp. 833–841, 2003. https://doi.org/10.1641/0006-3568(2003)053[0833:RAOPAM]2.0.CO;2.

[6] B. Soares-Filho, P. Moutinho, D. Nepstad, A. Anderson, H. Rodrigues, R. Garcia, L. Dietzsch, F. Merry, M. Bowman, and L. Hissa, "Role of Brazilian Amazon protected areas in climate change mitigation," *Proceedings of the National Academy of Sciences*, vol. 107, 2010.

[7] H. M. E. Alam, M. Y. Arafat, K. T. Ahmed, and M. N. Uddin, "Temporal variation of land surface temperature in response to changes in vegetation index of Bhawal National Park, Bangladesh," in *Lecture Notes in Civil Engineering*. Singapore: Springer, 2022, pp. 329–337. https://doi.org/10.1007/978-981-16-5543-2_27.

[8] M. M. Rahman, M. M. Rahman, Z. Guogang, and K. S. Islam, "A review of the present threats to tropical moist deciduous Sal (*Shorea robusta*) forest ecosystem of central Bangladesh," *Tropical Conservation Science*, vol. 3, no. 1, pp. 90–102, 2010. https://doi.org/10.1177/194008291000300108.

[9] E. Hasan and K. M. Bahauddin, "Community's perception and involvement in co-management of Bhawal National Park, Bangladesh," *Journal of Natural Sciences Research*, vol. 4, pp. 60–67, 2014.

[10] C.-R. Chang and M.-H. Li, "Effects of urban parks on the local urban thermal environment," *Urban Forestry and Urban Greening*, vol. 13, no. 4, pp. 672–681, 2014. https://doi.org/10.1016/j.ufug.2014.08.001.

[11] K. K. Islam and K. Hyakumura, "The potential perils of Sal forests land grabbing in Bangladesh: an analysis of economic, social and ecological perspectives," *Environment Development and Sustainability*, vol. 23, no. 1, pp. 1–23, 2021. https://doi.org/10.1007/s10668-021-01301-7.

[12] K. M. Masum, M. N. Islam, N. Saha, M. Z. Hasan, and A. Mansor, "Assessment of land grabbing from protected forest areas of Bhawal National Park in Bangladesh," *Landscape Research*, vol. 41, no. 3, pp. 330–343, 2015. https://doi.org/10.1080/01426397.2015.1078456.

[13] H. M. Abdullah, M. G. Mahboob, M. M. Rahman, and T. Ahmed, "Monitoring natural Sal forest cover in Modhupur, Bangladesh using temporal Landsat imagery during 1972–2015," *International Journal of Environment*, vol. 5, no. 1, pp. 1–7, 2015.

[14] R. Yesmin, A. S. M. Mohiuddin, M. J. Uddin, and M. A. Shahid, "Land use and land cover change detection at Mirzapur union of Gazipur district of Bangladesh using remote sensing and GIS technology," *IOP Conference Series: Earth and Environmental Science*, vol. 20, no. 1, 2014. https://doi.org/10.1088/1755-1315/20/1/012055.

[15] T. Shapla, J. Park, C. Hongo, and H. Kuze, "Agricultural land cover change in Gazipur, Bangladesh, in relation to local economy studied using Landsat images," *Advances in Remote Sensing*, vol. 4, no. 3, pp. 214–223, 2015.

[16] M. S. Iftekhar and A. K. F. Hoque, "Causes of forest encroachment: An analysis of Bangladesh," *GeoJournal*, vol. 62, pp. 95–106, 2005. https://doi.org/10.1007/s10708-005-7917-z.

[17] M. M. Ahsan, N. Aziz, and H. M. Morshed, "Management effectiveness assessment of protected areas of Bangladesh," SRCWP Project, Bangladesh Forest Department, 2016.

[18] G. S. Cumming and C. R. Allen, "Protected areas as social-ecological systems: Perspectives from resilience and social-ecological systems theory," *Ecological Applications*, vol. 27, pp. 1709–1717, 2017. https://doi.org/10.1002/eap.1584.

[19] J. Liu, H. Mooney, V. Hull, S. J. Davis, J. Gaskell, T. Hertel, J. Lubchenco, K. C. Seto, P. Gleick, C. Kremen, and S. Li, "Systems integration for global sustainability," *Science*, vol. 347, no. 6225, p. 1258832, 2015. https://doi.org/10.1126/science.1258832.

[20] C. Fuller, S. Ondei, B. W. Brook, and J. C. Buettel, "First, do no harm: A systematic review of deforestation spillovers from protected areas," *Global Ecology and Conservation*, vol. 18, p. e00591, 2019. https://doi.org/10.1016/j.gecco.2019.e00591.

[21] P. J. Ferraro and M. M. Hanauer, "Through what mechanisms do protected areas affect environmental and social outcomes?" *Philosophical Transactions of the Royal Society B: Biological Sciences*, vol. 370, no. 1681, p. 20140267, 2015. https://doi.org/10.1098/rstb.2014.0267.

[22] E. Ostrom, "A general framework for analyzing sustainability of social-ecological systems," *Science*, vol. 325, pp. 419–422, 2009. https://doi.org/10.1126/science.1172133.

[23] N. C. Ban, M. Mills, J. Tam, C. C. Hicks, S. Klain, N. Stoeckl, M. C. Bottrill, J. Levine, R. L. Pressey, T. Satterfield, and K. M. Chan, "A social-ecological approach to conservation planning: embedding social considerations," *Frontiers in Ecology and the Environment*, vol. 11, pp. 194–202, 2013. https://doi.org/10.1890/110205.

[24] D. L. A. Gaveau, J. Epting, O. Lyne, M. Linkie, I. Kumara, M. Kanninen, and N. Leader-Williams, "Evaluating whether protected areas reduce tropical deforestation in Sumatra," *Journal of Biogeography*, vol. 36, pp. 2165–2175, 2009. https://doi.org/10.1111/j.1365-2699.2009.02147.x.

[25] K. S. Andam, P. J. Ferraro, A. Pfaff, G. A. Sanchez-Azofeifa, and J. A. Robalino, "Measuring the effectiveness of protected area networks in reducing deforestation," *Proceedings of the National Academy of Sciences of the USA*, vol. 105, no. 42, pp. 16089–16094, 2008. https://doi.org/10.1073/pnas.0800437105.

[26] H. Balzter, B. Cole, C. Thiel, and C. Schmullius, "Mapping CORINE land cover from Sentinel-1A SAR and SRTM digital elevation model data using random forests," *Remote Sensing*, vol. 7, no. 11, pp. 14876–14898, 2015. https://doi.org/10.3390/rs71114876.

[27] P. S. Sharma and S. Roy, "Forest fragmentation in the Himalaya: A Central Himalayan case study," *International Journal of Sustainable Development & World Ecology*, vol. 14, pp. 201–210, 2007. https://doi.org/10.1080/13504500709469720.

[28] L. Gadrani, G. Lominadze, and M. Tsitsagi, "Assessment of land use/land cover (LULC) change of Tbilisi and surrounding area using remote sensing (RS) and GIS," *Annals of Agrarian Science*, vol. 16, no. 2, pp. 163–169, 2018. https://doi.org/10.1016/j.aasci.2018.02.005.

[29] K. A. Hossain, M. Masiero, and F. Pirotti, "Land cover change across 45 years in the world's largest mangrove forest (Sundarbans): The contribution of remote sensing in forest monitoring," *European Journal of Remote Sensing*, vol. 57, no. 1, 2022. https://doi.org/10.1080/22797254.2022.2097450.

[30] N. Chen, "Mapping mangrove in Dongzhaigang, China using Sentinel-2 imagery," *Journal of Applied Remote Sensing*, vol. 14, no. 01, p. 014508, 2020. https://doi.org/10.1117/1.JRS.14.014508.

[31] M. M. Rahman and H. Vacik, "Vegetation analysis and tree population structure of Sal (*Shorea robusta* C.F. Gaertn) forests: A case study from the Madhupur and Bhawal National Park in Bangladesh," in *National Parks: Vegetation, Wildlife and Threats*, O. Farina, Ed. New York: Nova Science Publishers, 2010.

[32] A. K. M. F. Huq and N. M. Sarker, "Country report on national parks, wildlife sanctuaries and game reserves of Bangladesh," prepared for the 25th Working Session of IUCN's Commission on National Parks and Protected Areas, India, 1985.

[33] D. S. Kabir and A. Z. Ahmed, "Wildlife biodiversity in Bhawal National Park: Management techniques and drawbacks of wildlife management and nature conservation," *Our Nature*, vol. 3, no. 1, 2006. https://doi.org/10.3126/on.v3i1.340.

[34] M. Belgiu and L. Drăguţ, "Random forest in remote sensing: A review of applications and future directions," *ISPRS Journal of Photogrammetry and Remote Sensing*, vol. 114, pp. 24–31, 2016. https://doi.org/10.1016/j.isprsjprs.2016.01.011.

[35] J. L. Speiser, M. E. Miller, J. Tooze, and E. Ip, "A comparison of random forest variable selection methods for classification prediction modeling," *Expert Systems with Applications*, vol. 134, pp. 93–101, 2019. https://doi.org/10.1016/j.eswa.2019.05.028.

[36] C. Zhang, I. Sargent, X. Pan, A. Gardiner, J. Hare, and P. M. Atkinson, "VPRS-based regional decision fusion of CNN and MRF classifications for very fine resolution remotely sensed images," *IEEE Transactions on Geoscience and Remote Sensing*, vol. 56, no. 8, pp. 4507–4521, 2018. https://doi.org/10.1109/TGRS.2018.2822783.

[37] M. I. Volke and R. Abarca-Del-Rio, "Comparison of machine learning classification algorithms for land cover change in a coastal area affected by the 2010 Earthquake and Tsunami in Chile," *Natural Hazards and Earth System Sciences*, 2020. https://doi.org/10.5194/nhess-2020-41.

[38] C. Gómez, J. C. White, and M. A. Wulder, "Optical remotely sensed time series data for land cover classification: A review," *ISPRS Journal of Photogrammetry and Remote Sensing*, vol. 116, pp. 55–72, 2016. https://doi.org/10.1016/j.isprsjprs.2016.03.008.

[39] J. Alzubi, A. Nayyar, and A. Kumar, "Machine learning from theory to algorithms: An overview," *Journal of Physics: Conference Series*, vol. 1142, p. 012012, 2018. https://doi.org/10.1088/1742-6596/1142/1/012012.

[40] E. C. Alex, K. V. Ramesh, and S. Hari, "Quantification and understanding the observed changes in land cover patterns in Bangalore," *International Journal of Civil Engineering and Technology*, vol. 8, no. 4, pp. 597–603, 2017.

[41] M. A. Quader, S. Agarwal, and M. Kervyn, "Multi-decadal land cover evolution in the Sundarban, the largest mangrove forest in the world," *Ocean & Coastal Management*, vol. 139, pp. 113–124, 2017. https://doi.org/10.1016/j.ocecoaman.2017.02.008.

[42] M. Özyavuz, C. Bilgili, and A. Salıcı, "Determination of vegetation changes with NDVI method," *Journal of Environmental Protection and Ecology*, vol. 16, no. 1, pp. 264–273, 2015.

[43] V. F. Rodriguez-Galiano, B. Ghimire, J. Rogan, and J. P. Rigol-Sanchez, "An assessment of the effectiveness of a random forest classifier for land-cover classification," *ISPRS Journal of Photogrammetry and Remote Sensing*, vol. 67, no. 1, pp. 93–104, 2012. https://doi.org/10.1016/j.isprsjprs.2011.11.002.

[44] H. M. Abdullah, I. Islam, M. G. Miah, and Z. Ahmed, "Quantifying the spatiotemporal patterns of forest degradation in a fragmented, rapidly urbanizing landscape: A case study of Gazipur, Bangladesh," *Remote Sensing Applications: Society and Environment*, vol. 13, pp. 457–465, 2019. https://doi.org/10.1016/j.rsase.2019.01.002.

[45] M. K. Ghosh, L. Kumar, and C. Roy, "Mapping long-term changes in mangrove species composition and distribution in the Sundarbans," *Forests*, vol. 7, no. 12, p. 305, 2016. https://doi.org/10.3390/f7120305.

[46] P. Sinha, L. Kumar, M. Drielsma, and T. Barrett, "Time-series effective habitat area (EHA) modeling using cost-benefit raster based technique," *Ecological Informatics*, vol. 19, pp. 16–25, 2014. https://doi.org/10.1016/j.ecoinf.2013.10.003.

[47] R. G. Congalton and K. Green, *Assessing the Accuracy of Remotely Sensed Data: Principles and Practices*, 3rd ed. 2019. https://doi.org/10.1201/9780429052729.

[48] K. D. Kanniah, A. Sheikhi, A. P. Cracknell, H. C. Goh, K. P. Tan, C. S. Ho, and F. N. Rasli, "Satellite images for monitoring mangrove cover changes in a fast growing economic region in Southern Peninsular Malaysia," *Remote Sensing*, vol. 7, no. 11, pp. 14360–14385, 2015. https://doi.org/10.3390/rs71114360.

[49] S. V. Stehman, "Estimating the Kappa coefficient and its variance under stratified random sampling," *Photogrammetric Engineering and Remote Sensing*, vol. 62, pp. 401–407, 1996.

[50] S. S. Rwanga and J. M. Ndambuki, "Accuracy assessment of land use/land cover classification using remote sensing and GIS," *International Journal of Geosciences*, vol. 8, no. 4, pp. 611–622, 2017. https://doi.org/10.4236/ijg.2017.84033.

[51] J. R. Jensen, *Introductory Digital Image Processing: A Remote Sensing Perspective*, 3rd ed. Upper Saddle River, NJ: Prentice Hall, 2004.

[52] S. Z. Aldwaik and R. G. Pontius, "Intensity analysis to unify measurements of size and stationarity of land changes by interval, category, and transition," *Landscape and Urban Planning*, vol. 106, no. 1, pp. 103–114, 2012. https://doi.org/10.1016/j.landurbplan.2012.02.010.

[53] E. Teferi, W. Bewket, S. Uhlenbrook, and J. Wenninger, "Understanding recent land use and land cover dynamics in the source region of the Upper Blue Nile, Ethiopia: Spatially explicit statistical modeling of systematic transitions," *Agriculture, Ecosystems & Environment*, vol. 165, pp. 98–117, 2013. https://doi.org/10.1016/j.agee.2012.11.007.

[54] M. W. A. Halmy, P. E. Gessler, J. A. Hicke, and B. B. Salem, "Land use/land cover change detection and prediction in the north-western coastal desert of Egypt using Markov-CA," *Applied Geography*, vol. 63, pp. 101–112, 2015. https://doi.org/10.1016/j.apgeog.2015.06.015.

[55] W. Zewdie and E. Csaplovics, "Identifying categorical land use transition and land degradation in northwestern drylands of Ethiopia," *Remote Sensing*, vol. 8, p. 408, 2016. https://doi.org/10.3390/rs8050408.

[56] P. Vogt, K. H. Riitters, and C. Estreguil, "Mapping spatial patterns with morphological image processing," *Landscape Ecology*, vol. 22, pp. 171–177, 2007. https://doi.org/10.1007/s10980-006-9013-2.

[57] K. McGarigal, S. A. Cushman, M. C. Neel, and E. Ene, *FRAGSTATS: Spatial Pattern Analysis Program for Categorical Maps.* Computer software program produced by the authors at the University of Massachusetts, Amherst, January 2002. Available: http://www.umass.edu/landeco/research/fragstats/fragstats.html.

[58] D. R. G. MacLean and M. G. Congalton, "Mapping and analysis of fragmentation in Southeastern New Hampshire," in *A Special Joint Symposium of ISPRS Technical Commission IV and AutoCarto, ASPRS/CaGIS 2010 Fall Specialty Conference*, Orlando, Florida, 2010.

[59] M. Batistella, E. S. Brondizio, and E. F. Moran, "Comparative analysis of landscape fragmentation in Rondônia, Brazilian Amazon," *International Archives of Photogrammetry and Remote Sensing*, vol. XXXIII, part B7, Amsterdam, 2000.

[60] G. R. Jaybhaye, K. P. Kale, and P. Joshi, "The relevance of geospatial techniques in the assessment of forest fragmentation of Anjaneri Hill, Nasik District, Maharashtra, India," *Journal of Environmental Science, Toxicology and Food Technology*, vol. 10, no. 4, pp. 01–10, 2016. https://doi.org/10.9790/2402-1004010110.

[61] S. Paudel and F. Yuan, "Assessing landscape changes and dynamics using patch analysis and GIS modeling," *International Journal of Applied Earth Observation and Geoinformation*, vol. 16, pp. 66–76, 2012. https://doi.org/10.1016/j.jag.2011.12.003.

[62] B. Flowers, K.-T. Huang, and G. O. Aldana, "Analysis of the habitat fragmentation of ecosystems in Belize using landscape metrics," *Sustainability*, vol. 12, p. 3024, 2020. https://doi.org/10.3390/su12073024.

[63] J. R. Landis and G. G. Koch, "The measurement of observer agreement for categorical data," *Biometrics*, vol. 33, p. 159, 1977. https://doi.org/10.2307/2529310.

[64] D. Lu and Q. Weng, "A survey of image classification methods and techniques for improving classification performance," *International Journal of Remote Sensing*, vol. 28, no. 5, pp. 823–870, 2007. https://doi.org/10.1080/01431160600746456.

[65] A. K. Batar, T. Watanabe, and A. Kumar, "Assessment of land-use/land-cover change and forest fragmentation in the Garhwal Himalayan region of India," *Environments*, vol. 4, no. 2, p. 34, 2017. https://doi.org/10.3390/environments4020034.

[66] S. Budiharta, E. Meijaard, J. A. Wells, and K. A. Wilson, "Enhancing feasibility: Incorporating a socio-ecological systems framework into restoration planning," *Environmental Science & Policy*, vol. 64, pp. 83–92, 2016. https://doi.org/10.1016/j.envsci.2016.06.014.

[67] R. Gregory, L. Failing, M. Harstone, G. Long, T. McDaniels, and D. Ohlson, *Structured Decision Making: A Practical Guide to Environmental Management Choices.* West Sussex, UK: John Wiley & Sons, 2012. https://doi.org/10.1002/9781444398557.